

# QCD Saturation and Photoproduction on Proton and Nuclei Targets

J. Bartels, \* <sup>a)</sup> E. Gotsman, <sup>†</sup> <sup>b), d)</sup> E. Levin, <sup>‡</sup> <sup>b), c)</sup> M. Lublinsky, <sup>§</sup> <sup>c)</sup>  
and U. Maor <sup>¶</sup> <sup>b)</sup>

<sup>a)</sup> *II Institut für Theoretische Physik,  
Universität Hamburg, D-22761 Hamburg, GERMANY*

<sup>b)</sup> *HEP Department School of Physics and Astronomy  
Raymond and Beverly Sackler Faculty of Exact Science  
Tel Aviv University, Tel Aviv, 69978, ISRAEL*

<sup>c)</sup> *DESY Theory Group  
22607, Hamburg, GERMANY*

<sup>d)</sup> *Department of Physics and Astronomy  
University of California, Irvine, CA 92612, USA*

June 26, 2018

## Abstract

We calculate inclusive photoproduction cross-sections for both proton and nuclei targets, using a saturation model derived from an approximate solution to the Balitsky-Kovchegov nonlinear evolution equation. This paper extends our hypothesis, that one can successfully use the dipole picture and saturation models to describe soft processes, instead of the soft Pomeron Regge parametrization. Our fit is compatible with our previous fit to DIS data, and utilizes the same phenomenological parameters as in our paper devoted to soft hadronic interactions. Using the Glauber formalism, and no additional parameters, we calculate the cross-sections for photoproduction on various nuclei, and compare our results with the relevant data.

---

\*e-mail: jochen.bartels@desy.de

<sup>†</sup>e-mail: gotsman@post.tau.ac.il

<sup>‡</sup>e-mail: leving@post.tau.ac.il; levin@mail.desy.de

<sup>§</sup>e-mail: lublinm@mail.desy.de; mal@tx.technion.ac.il

<sup>¶</sup>e-mail: maor@post.tau.ac.il

# 1 Introduction

Over the past few years there has been much progress in the successful application of perturbative QCD to DIS processes for values of  $Q^2 \geq 2 \text{ GeV}^2$ . For very small  $Q^2$ , Regge theory (e.g.[1]) provides a reasonable description of the data. Attempts have been made to bridge the two  $Q^2$  regions, using methods incorporating high parton densities and saturation. Models based upon these ideas have lead to excellent descriptions of the DIS cross-section for all values of  $Q^2$  and  $x \leq 0.01$  [2, 3, 4]. The saturation hypothesis has been successfully applied to  $\gamma - \gamma$  scattering in Ref. [5]. In our recent paper [6] we showed that QCD-based saturation models can lead to satisfactory descriptions of cross sections in soft hadron-hadron interactions.

A pioneering attempt to apply the dipole picture and the physics of high parton densities to photoproduction ( $Q^2 = 0$ ) processes was made by Golec-Biernat and Wusthoff (GBW) within the framework of their saturation model [2]. Our goal is to investigate further to what precision high energy photoproduction can be described using the saturation hypothesis. We use a saturation model based on a solution of the nonlinear evolution equation [7]. We also extend our analysis to the case of nuclei targets.

The hypothesis of saturation refers to the interactions between partons from different cascades, which are omitted in the linear evolution equations (DGLAP and BFKL), and which become more significant with increasing energy. The parton saturation phenomenon introduces a characteristic momentum scale  $Q_s(x)$ , which is a measure of the density of the saturated gluons. It grows rapidly with energy, and it is proportional to  $\frac{1}{x^\lambda}$  [2, 4, 8, 9, 10] with  $\lambda \simeq 0.2$ . Parton saturation effects are expected to be relevant at low values of  $Q^2$  and  $x$ , where the parton densities are sufficiently large.

The starting point of this endeavour is the successful fit [4] within the framework of QCD, to the  $F_2$  structure function data for all values of  $Q^2$  and  $x \leq 0.01$ . This was achieved by using an approximate solution to the Balitsky-Kovchegov (BK) [7] nonlinear evolution equation, and adding a correcting function to improve the DGLAP behaviour at large  $Q^2$ . Although soft physics was not explicitly included, agreement with experiment was found for all quantities associated with  $F_2$ , in particular for the logarithmic slope  $\lambda \equiv \partial \ln F_2 / \partial (\ln 1/x)$ , where a value of  $\lambda \approx 0.08$  was obtained for very low  $x$  and  $Q^2$  well below  $1 \text{ GeV}^2$ , i.e. in the saturation region. This value is identical to that of the intercept of the "soft" Pomeron, associated with the Donnachie-Landshoff (DL) model [11].

In this paper we further pursue the hypothesis that colour dipoles are the correct degrees of freedom in photoproduction scattering processes at high energy, even when large transverse distances come into play. We adopt the well known expression for the DIS cross-sections

$$\sigma^{\gamma^*p}(x, Q^2) = \int d^2r_\perp dz P^{\gamma^*}(Q^2, r_\perp, z) \sigma_{dipole}(x, r_\perp), \quad (1.1)$$

where  $Q^2$  is the virtual photon's four momentum squared.  $P^{\gamma^*}$  denotes the probability of finding a  $q - \bar{q}$  colour dipole with transverse separation  $r_\perp$  inside the photon.  $s = W^2$  is the energy squared in the photon-proton system and  $z$ ,  $(1 - z)$  the momentum fraction taken by the quark (antiquark) respectively,  $x = \frac{Q^2}{(W^2 + Q^2)}$ . The dipole cross-section  $\sigma_{dipole}$  describes the interaction of the  $q\bar{q}$  pair with the proton target. The exact form of this cross-section has not yet been determined. GBW [2] proposed a very successful parametrization for  $\sigma_{dipole}$ . In our approach  $\sigma_{dipole}$  is obtained by solving the nonlinear evolution equation, which is derived in QCD.

In [4] the nonlinear evolution equation with certain approximations, was solved numerically, the initial conditions were determined by fitting to the low  $x$  DIS data. In this paper the resulting

parametrization for  $\sigma_{dipole}$  is adopted for the case of photoproduction. In contrast to our treatment of the DIS case [4], we need to introduce additional nonperturbative parameters to insure a finite result in the limit  $Q^2 \rightarrow 0$ . This leads to a successful description of both the photoproduction and low  $Q^2$  DIS data. Our approach for photoproduction is very similar to that which we employed for soft hadronic interactions in Ref. [6].

As a further test of our hypothesis we apply our model to the case of the photon scattering on nuclei targets. This extension does not involve any additional parameters, and can thus be regarded as an independent check. All available data on nuclear shadowing is successfully reproduced for heavy nuclei. An approach similar to the one presented here for the photon scattering on nuclei can be found in Ref. [12]. In [12] a Glauber formula with the GBW model was used. In this paper, we rely on the model defined in Ref. [4].

The content of the paper is as follows. In Section 2 we discuss the numerical solution of the BK equation [7]. We briefly review the GBW saturation model [2], with which we compare some of our results. In Section 3 we present the changes that must be introduced to adapt the formalism for the calculation of photoproduction cross-sections. Section 4 is devoted to the overall picture, including comparison of the model's results with experimental data. We extend our approach to nuclei targets in Section 5. Section 6 contains a discussion of our results and our conclusions.

## 2 Description of the Saturation Models

In [4] an approximate solution to the BK non-linear evolution equation [7] was obtained using numerical techniques. Below we briefly review the method used and the main results obtained. For more details of the method of solution we refer to [4].

The solution of the BK equation which we denote by  $\tilde{N}$ , takes into account the collective phenomena of high parton density QCD. Starting from an initial condition which contains free parameters, we have numerically solved the nonlinear evolution equation, restricting ourselves to the point  $b_\perp = 0$ . The parameters which appear in the initial conditions, have been determined by fitting to the  $F_2$  data [4], and the resulting approximate solution is displayed in Fig. 1.

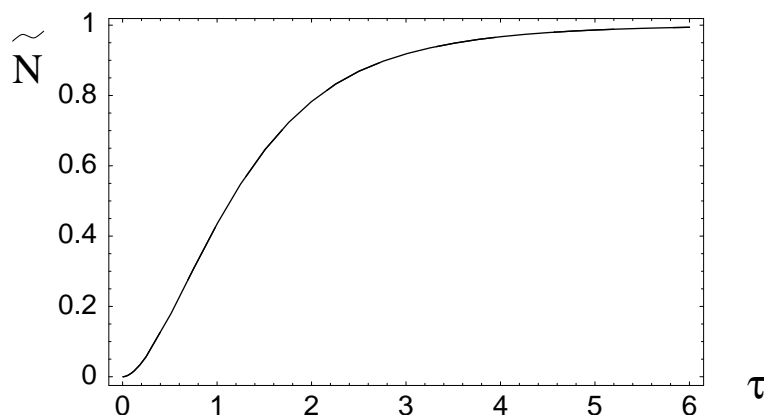


Figure 1:  $\tilde{N}(b_\perp = 0)$  versus  $\tau = r_\perp Q_s(x)$ .

The  $b_\perp$ -dependence of the solution is restored using the ansatz:

$$\tilde{N}(r_\perp, x; b_\perp) = (1 - e^{-\kappa(x, r_\perp) S(b_\perp)}), \quad (2.1)$$

where  $\kappa$  is related to the  $b_\perp = 0$  solution

$$\kappa(x, r_\perp) = -\ln(1 - \tilde{N}(r_\perp, x, b_\perp = 0)). \quad (2.2)$$

A Gaussian form for the profile function in impact parameter space was taken as

$$S(b_\perp) = \frac{1}{\pi R_{proton}^2} \exp\left(-\frac{b_\perp^2}{R_{proton}^2}\right). \quad (2.3)$$

where  $R_{proton}^2 = 3.1 \text{ GeV}^{-2}$  refers to the radius of the target proton. Our choice of a Gaussian profile function simplifies the numerical calculations. It was shown [13] that calculations pertaining to total and integrated cross-sections are insensitive to the details of the profile function, unlike the case for differential quantities.

The dipole-proton cross-section (from eq.(2.4) of [4]) is given by:

$$\sigma_{dipole}(r_\perp, x) = 2 \int d^2 b_\perp \tilde{N}(r_\perp, b_\perp, x). \quad (2.4)$$

The contribution of the  $F_2$  structure function is

$$\tilde{F}_2(x, Q^2) = \frac{Q^2}{4\pi^2} \int d^2 r_\perp \int dz P^{\gamma*}(Q^2; r_\perp, z) \sigma_{dipole}(r_\perp, x). \quad (2.5)$$

The physical content of Eq. (2.5) is easily explained. It describes the two stages of DIS [14]. The first stage is the decay of a virtual photon into a colorless dipole ( $q\bar{q}$ -pair), the probability of this decay is given by  $P^{\gamma*}$ . The second stage is the interaction of the dipole with the target i.e. ( $\sigma_{dipole}$  in Eq. (2.5)). This equation is a simple manifestation of the fact that color dipoles are the correct degrees of freedom in QCD at high energies [15]. The probability  $P^{\gamma*}$  is given by the square of the QED wave functions of the virtual photon, which are well known [15, 16, 17]:

$$P^{\gamma*}(Q^2; r_\perp, z) = \frac{N_c}{2\pi^2} \sum_f Z_f^2 \times \left\{ (z^2 + (1-z)^2) a^2 K_1^2(ar_\perp) + m_q^2 K_0^2(ar_\perp) + 4Q^2 z^2 (1-z)^2 K_0^2(ar_\perp) \right\}, \quad (2.6)$$

with  $a^2 = Q^2 z(1-z) + m_q^2$ .

In Ref. [4] we assumed the mass of the quark to be zero i.e. we took  $m_q = 0$  in the above equation. The structure function  $F_2$  is given by a sum of three contributions:

$$F_2 = \tilde{F}_2 + \Delta F + F_2^{NSQ}, \quad (2.7)$$

where the first term is given by Eq. (2.5). The second term is a DGLAP (large  $Q^2$ ) correction to  $\tilde{F}$  and is of no importance for the present analysis. These two terms take into account the gluon contribution to  $F_2$ . Gluons are related to the singlet quark distributions. The third term in (2.7) includes contributions of non-singlet quark distributions:

$$F_2^{NSQ} = \sum_{i=u,d} e_i^2 q_i^V. \quad (2.8)$$

At the present stage of our investigation we "borrow" the valence quark distributions ( $q_i^V$ ) from the LO CTEQ6 parametrization [18]. It is important to note that these distributions decrease

with decreasing  $x$ , and are practically of no significance below  $x \simeq 10^{-3}$ . As the valence quark parametrization is not given below some scale of order  $1 \text{ GeV}^2$ , for low photon virtualities we freeze the valence quark distribution at its  $Q^2 = 1 \text{ GeV}^2$  value.

A popular saturation model was proposed by GBW [2]. In this model the dipole cross-section is taken as

$$\hat{\sigma}_{dipole}(r_{\perp}, x) = \sigma_0 \left[ 1 - \exp\left(-\frac{r_{\perp}^2}{4R_0^2}\right) \right] \quad (2.9)$$

, with  $R_0^2(x)[\text{GeV}^{-2}] = (\frac{x}{x_0})^{\lambda}$ . The values of the parameters which were determined by fitting to DIS data at HERA for  $x \leq 0.01$ , are:  $\sigma_0 = 23 \text{ mb}$ ,  $\lambda = 0.29$  and  $x_0 = 3 \times 10^{-4}$ . The  $r_{\perp}$  dependence was taken as Gaussian, which leads to a constant-cross section  $\sigma_0$  for large  $r_{\perp}^2$  (or small  $Q^2$ ).

The dipole cross-section of the GBW saturation model and  $\tilde{N}$  are closely related. Both models take into account gluon saturation, preserve unitarity, and describe the physics associated with "long distances". Whereas  $\tilde{N}$  has its origins in QCD,  $\hat{\sigma}_{dipole}$  is phenomenological.

There are differences between the two models. Unlike the GBW  $\hat{\sigma}_{dipole}$ , the dipole cross-section obtained from the solution of the BK equation is not saturated as a function of  $x$ . With the assumed Gaussian profile function, the integration over impact parameter  $b_{\perp}$  leads to a logarithmic growth with decreasing  $x$ .

### 3 Details of Our Calculation

In Ref. [4] we considered a massless ( $m_q = 0$ ) case only. To proceed to the limit  $Q^2 \rightarrow 0$  we need to introduce a finite mass as a cutoff for the  $r_{\perp}$  integration in Eq. (2.5). It is important to stress, however, that we do not modify the dipole cross section  $\sigma_{dipole}$  (2.4), which was constructed in [4] from a fit to the  $F_2$  data. Since  $x$  is not defined for photoproduction, to relate  $x$  to the energy of the process we need to introduce an additional nonperturbative scale, denoted as  $Q_0^2$ . Though these two parameters are not obviously related, we set  $Q_0^2 = 4 m_q^2$ . We redefine  $x$  as

$$x = (Q^2 + Q_0^2)/W^2; \quad s = W^2, \quad (3.1)$$

and use  $m_q$  as a fitting parameter for high energy photoproduction. The energy dependence of the photoproduction cross section enters only through the  $x$ -dependence of the dipole cross section, the later being adjusted or constructed to describe DIS data of the  $F_2$  structure function.

Note that having introduced these modifications we alter the results in low  $Q^2$  domain. This can potentially spoil our original fit [4]. Thus photoproduction should be considered simultaneously with DIS. The fit to the later should not be affected by the introduction of new parameters.

To obtain a finite result in the limit  $Q^2 \rightarrow 0$ , GBW [2] introduce the quark mass as a regulator, and assume a common mass of 140 MeV for the three light quarks, "which leads to a reasonable prediction in the photoproduction region". We refer the reader to [2] for details of the GBW model, in this paper we use the GBW model only to compare with our results for photoproduction on nuclear targets.

In the colour dipole picture, one can hopefully reproduce only the asymptotic energy dependence i.e. the Pomeron contribution. The solution to the BK equation is also used to model this vacuum exchange channel in the nonperturbative domain. Thus parton-hadron duality is used in this approach. At lower energies where most of the photoproduction data are available, there are

also contributions from nonvacuum exchanges. The evaluation of these contributions is beyond the scope of our model.

In [4] the contribution of the nonsinglet exchange was represented by the valence quarks. Since the latter were frozen at  $Q^2 = 1 \text{ GeV}^2$ , their contribution to the cross section would have the wrong dependence at  $Q^2 \rightarrow 0$  (become infinite). An improved form for this contribution of the valence quarks below  $1 \text{ GeV}^2$  is:

$$F_2^{NSQ} = \frac{(Q^2)^{1+\beta}}{1 (\text{GeV}^2)^{1+\beta}} \frac{(1 \text{ GeV}^2 + \mu^2)}{Q^2 + \mu^2} \sum_{i=u,d} e_i^2 q_i^V(Q^2 = 1 \text{ GeV}^2). \quad (3.2)$$

Vector current conservation requires  $\beta \geq 0$ , in principle, both  $\beta$  and  $\mu$  are fitting parameters. This freedom was not used in [4] where  $\beta = 0$  and  $\mu^2 \rightarrow 0$ . The energy dependence of the valence quark contribution enters through its  $x$ -dependence, which is frozen at  $Q^2 = 1 (\text{GeV}^2)$ . Taking  $\mu$  as a fitting parameter produces a good description of both the DIS and photoproduction data (keeping  $\beta = 0$ ).

In our approach we use parton-hadron duality in two ways. For the vacuum exchange we assume that the saturation result, which was derived for large  $Q^2$  virtualities, is a valid description (on average) of the cross section at small values of  $Q^2$ . For the contribution of the non-singlet structure function we can use a parametrization that is successful for soft interactions, namely the exchange of secondary Reggeons. We believe that this exchange can be used for larger  $Q^2$  (up to  $1 \text{ GeV}^2$ ). In the spirit of Ref. [11, 19] and using Gribov's formula [14] the secondary Reggeon contribution is

$$\left(\frac{s}{s_0}\right)^{\alpha_R} \int \frac{dM^2 \rho(M^2)}{Q^2 + M^2} g_R(M^2), \quad (3.3)$$

where  $\rho(M^2)$  is related to the cross section for  $e^+e^-$  annihilation while  $g_R$  is a residue of the secondary trajectory. We approximate (3.3) by the following contribution

$$\sigma^{\gamma p} \sim f(0) \frac{\tilde{M}^2}{(Q^2 + \tilde{M}^2)} (s/s_0)^{\alpha_R}; \quad \alpha_R = -0.45; \quad s_0 = 1 (\text{GeV}^2). \quad (3.4)$$

$f(0)$  is the residue at  $Q^2 = 0$ , and is determined by fitting to the low energy photoproduction data.  $\tilde{M}$  is an additional fitted parameter.

## 4 Photoproduction and DIS at low $Q^2$

A fit to high energy photoproduction data yields the value of

$$m_q = 0.15 \text{ GeV}.$$

Note that we obtain practically the same quark mass as GBW [2].

As most of the photoproduction data was measured at lower energies, it is essential to include an additional component which is dominant in this energy range. We attempt two alternative parametrizations for this component.

The first is based on the Regge pole model Eq.(3.4) which we denote:

- **Model ST:** In this model there are two parameters to be fitted which determine the contribution of the non-leading (or secondary trajectories) to the DIS cross-section (see Eq. (3.4)). These are

$$f(0) = 0.19 \text{ mbarn}; \quad \tilde{M}^2 = 2 \text{ GeV}^2.$$

The cross section obtained with these parameter values is indicated by the dashed curve in Figs. 2, 3. The second parametrization is based on the quark model:

- **Model VQ:** This alternate method of accounting for the non-singlet contribution to the DIS cross-section is via the valence quarks (see Eq. (3.2)). There are also two free parameters here, whose values are determined by fitting to the data. These are

$$\beta = 0 \text{ (kept fixed)}; \quad \mu^2 = 0.13 \text{ GeV}^2.$$

The resulting photoproduction cross section with this parametrization for the valence quarks is shown as the full line in Figs. 2, 3.

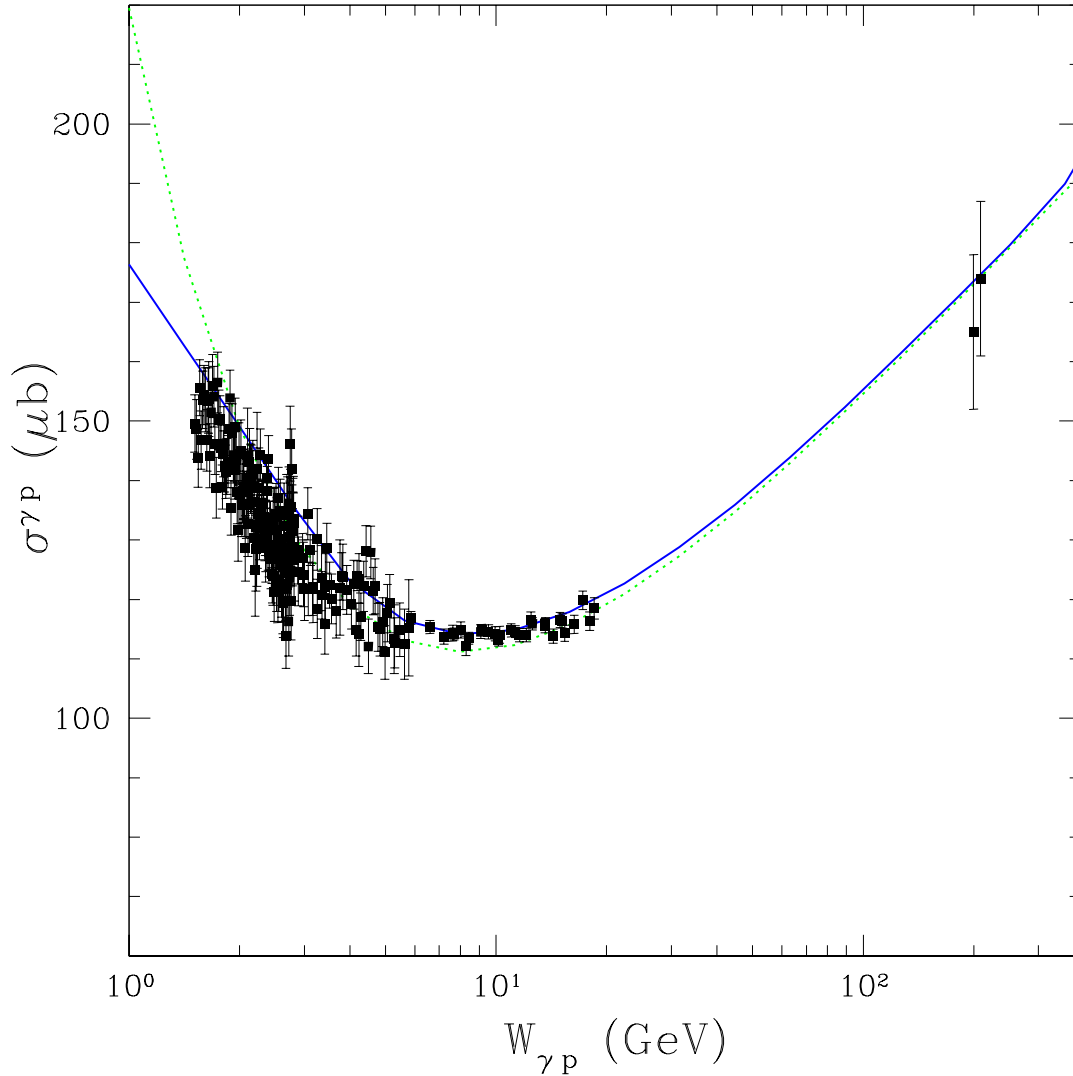


Figure 2: Photoproduction as a function of  $\gamma - p$  energy. Preliminary data from [20]. The solid line indicates the results of Model VQ, while the dashed line those of Model ST.

We note an interesting duality between the two models, both produce reasonable descriptions of the experimental measurements (see Fig. 2), including the low energy photoproduction data. For the case of a proton target we do not present a comparison with the GBW model, since the later was formulated only for high energies and does not include any contribution of secondary trajectories.

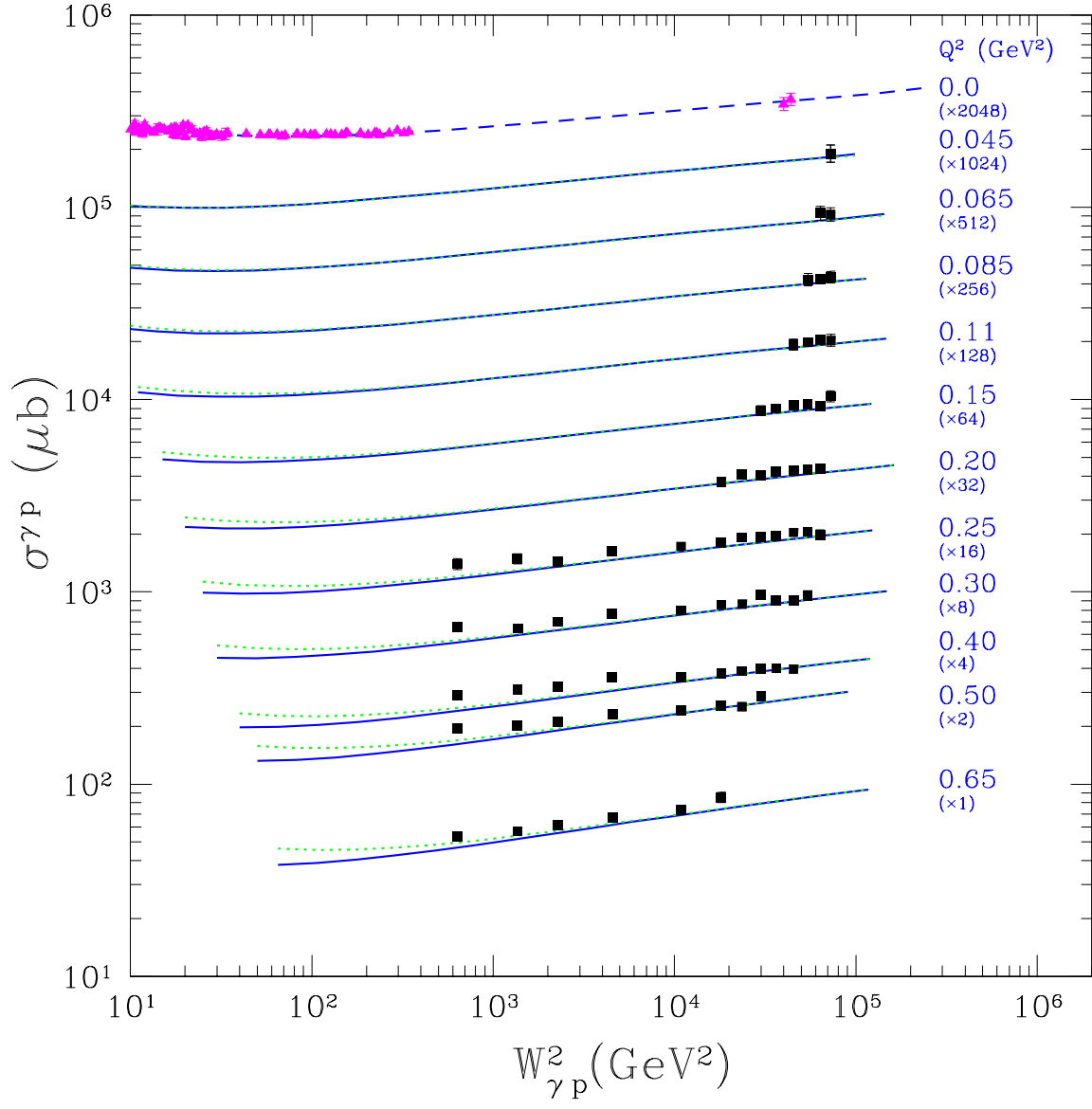


Figure 3: DIS cross section at very low  $Q^2$ . The two curves correspond to two different models for the secondary trajectory (see text). Data from [21].



## 5 Photoproduction on Nuclei

In our approach we obtain a very small effective radius of the nucleon. The consequence of such a small radius is that the typical parameter that governs the dipole interaction with the nuclear target, is also very small, namely

$$\pi R_{proton}^2 S_A(0) \leq 1 \quad \text{for } A \leq 200, \quad (5.1)$$

where  $S_A(b_\perp)$  denotes the Wood-Saxon impact parameter distribution of the nucleons in a nucleus. In the standard approach,  $\pi R_{proton}^2 S_A(0)$  is considered to be large. Instead of one equation [7], Eq. (5.1) leads to a set of non-linear equations which have to be formulated and solved. Before doing so it is necessary to determine the  $b_\perp$  distribution for dipole-nucleon scattering, which is still an ansatz in our approach. At present, the best that we can do is to extend the Glauber formalism which takes into account all rescatterings inside the nucleus. This approach is certainly correct at not too high energies, however to determine the region of applicability we need to solve the explicit set of equations.

The Glauber formula has a familiar form:

$$\sigma(\gamma^* A \longrightarrow \gamma^* A) = \int d^2 b_\perp \int dz d^2 r_\perp P^{\gamma^*}(r_\perp, z, Q^2) 2 \left( 1 - e^{-\frac{\sigma_{dipole}}{2} S_A(b_\perp)} \right). \quad (5.2)$$

In our model  $\sigma_{dipole}$  is given by Eq. (2.4). We use the GBW model for the dipole cross section for comparison (see also Ref. [12] for a similar analysis).

As discussed previously, at low energies we need to add contributions of the secondary trajectories. For the Glauber approach the  $A$  dependence of the secondary trajectory can be estimated as follows:

$$A_{eff}^{st}(x) = \int d^2 r_\perp |\Psi_\pi(r_\perp)|^2 \int d^2 b_\perp S_A(b_\perp) e^{-\frac{\sigma_{dipole}(r_\perp, x)}{2} S_A(b_\perp)}. \quad (5.3)$$

Here  $\Psi_\pi$  denotes the pion wave function. For  $\Psi_\pi$  we use a simple Gaussian parametrization taken from Ref. [22]. The physical meaning and the derivation of Eq. (5.3) is clear from Fig. 4. Indeed, the exchange of secondary Regge trajectories is screened by the black disc type interaction in the vacuum channel (the two diagrams in Fig. 4 which cancel each other at small  $b_\perp$ ). The factor  $\exp(-\sigma_{dipole} S(b_\perp)/2)$  is the probability that the dipole does not have any inelastic interaction (for a more detailed discussion see Ref. [23]).

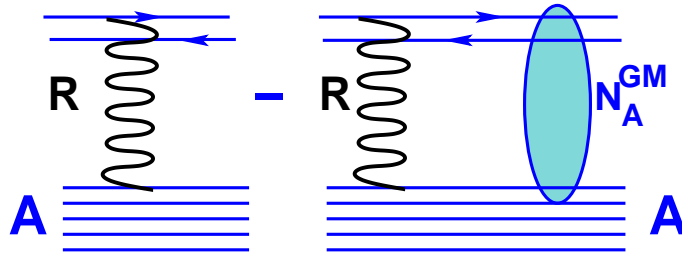


Figure 4: The diagrams for the secondary reggeon interaction with nuclei.  $N_A^{GM}$  is the dipole-nucleus amplitude in the Glauber-Mueller approach. The two diagrams cancel each other and lead to Eq. (5.3).

We compute the total cross section for  $\gamma - A$  collision as a sum of two terms

$$\sigma(\gamma^* A) = Eq. (5.2) + A_{eff}^{st} \times Eq. (3.4). \quad (5.4)$$

Figs. 5, 6 7 illustrate the dependence of  $A_{eff} = \sigma(\gamma^*A)/\sigma(\gamma^*p)$  as a function of  $x$  for different values of the photon virtuality  $Q^2$  for photo scattering on Pb, Xe, and Ca respectively. Fig. 8 shows a comparison for  $F_2$  on Ca. The data sets have a few percents overall normalization uncertainty.

In the figures below we use the following notation: the solid line shows the results of our formalism, where  $\sigma_{dipole}$  in Eq. (5.2) is calculated from the solution of the non-linear equation. The dotted line illustrates the Glauber approximation for the GBW model for the dipole-nucleon cross section, without a secondary Regge pole contribution.<sup>1</sup>

Agreement with experimental data for both dipole models is good. A comparison of our model prediction for a lead target with the results other models can be found in the recent preprint [24].

In Fig. 9 we plot the  $x$  dependence of  $\alpha$  for the parametrization  $\sigma(\gamma^*A) \propto A^\alpha$ . Compared to GBW our results appear to be in slightly better agreement with the data. However, the data are not precise enough to really distinguish between the two models.

Our prediction for the  $Q^2$  dependence of  $\alpha$  is shown in Fig. 10.

We compare the predictions for the energy behaviour of our approach with the relevant data for  $A_{eff}/A$  for photoproduction on Pb in Fig. 11, and on Cu in Fig. 12. We slightly underestimate the data for Pb case, and are consistent with the Cu measurements. Some points of the Caldwell data (1979) [28] are read off the plots and divided by our photoproduction cross section.

The curves in Fig. 13 which show predictions for the values of the total  $\gamma^*A$  cross section are crucial as a check of our approach. The results of both models are very close and this boosts our confidence in our calculations. The predictions for  $F_2$  for  $\gamma^*$  - gold scattering for both approaches are given in Fig. 14, again the results are close to one another.

## 6 Discussion and Conclusions

This paper demonstrates that assuming QCD saturation of the parton densities at high energies, one is able to describe photoproduction processes, as well as DIS at small values of photon virtuality. We establish that the revised parametrization does not spoil the predictions made for DIS processes at large and moderate values of  $Q^2$ . This is important as it allows us to use the DIS data to fix the phenomenological parameters of our approach.

As in our treatment of the soft hadron interactions in Ref. [6], the present analysis is based on two parameters and two major assumptions. The parameters are:

- (a) The effective radius of proton which is taken from the description of the DIS data for  $x < 10^{-2}$ ;
- (b) The parameter  $Q_0^2$ , (introduced in Eq. (3.1)), is adjusted by comparing with the high energy photoproduction data.

The two assumptions are:

- (i) We use Eq. (2.1) as an ansatz for the  $b_\perp$ -dependence. This Glauber-type  $b_\perp$  dependence has no solid theoretical foundation and should be considered to be an initial guess. It is therefore reassuring to see that our successful description of the photoproduction data is in reasonable agreement with this ansatz;
- (ii) We use hadron-parton duality to introduce the contribution of the secondary Regge trajectories. The result that the contribution of the secondary reggeons is dual to the valence quark one, is unexpected and interesting.

---

<sup>1</sup>In principle, contributions of the secondary trajectories should be added to the GBW model as well.

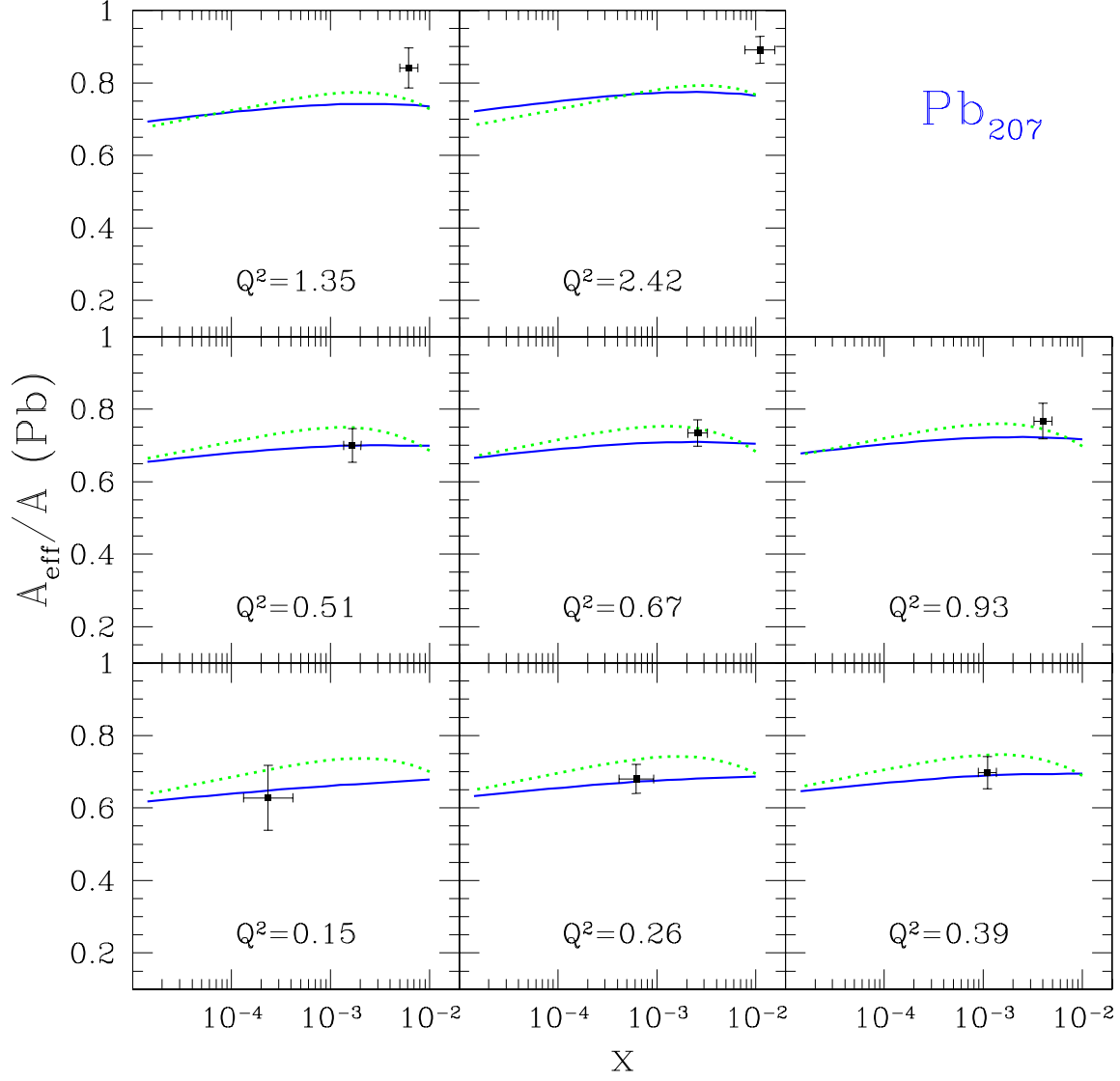


Figure 5:  $A_{eff}/A$  on a Pb target. The solid line denotes the results of our model including a secondary Regge contribution. The dotted line is the result for the Glauber approx. for GBW model without a secondary Regge contribution. Data from [25].

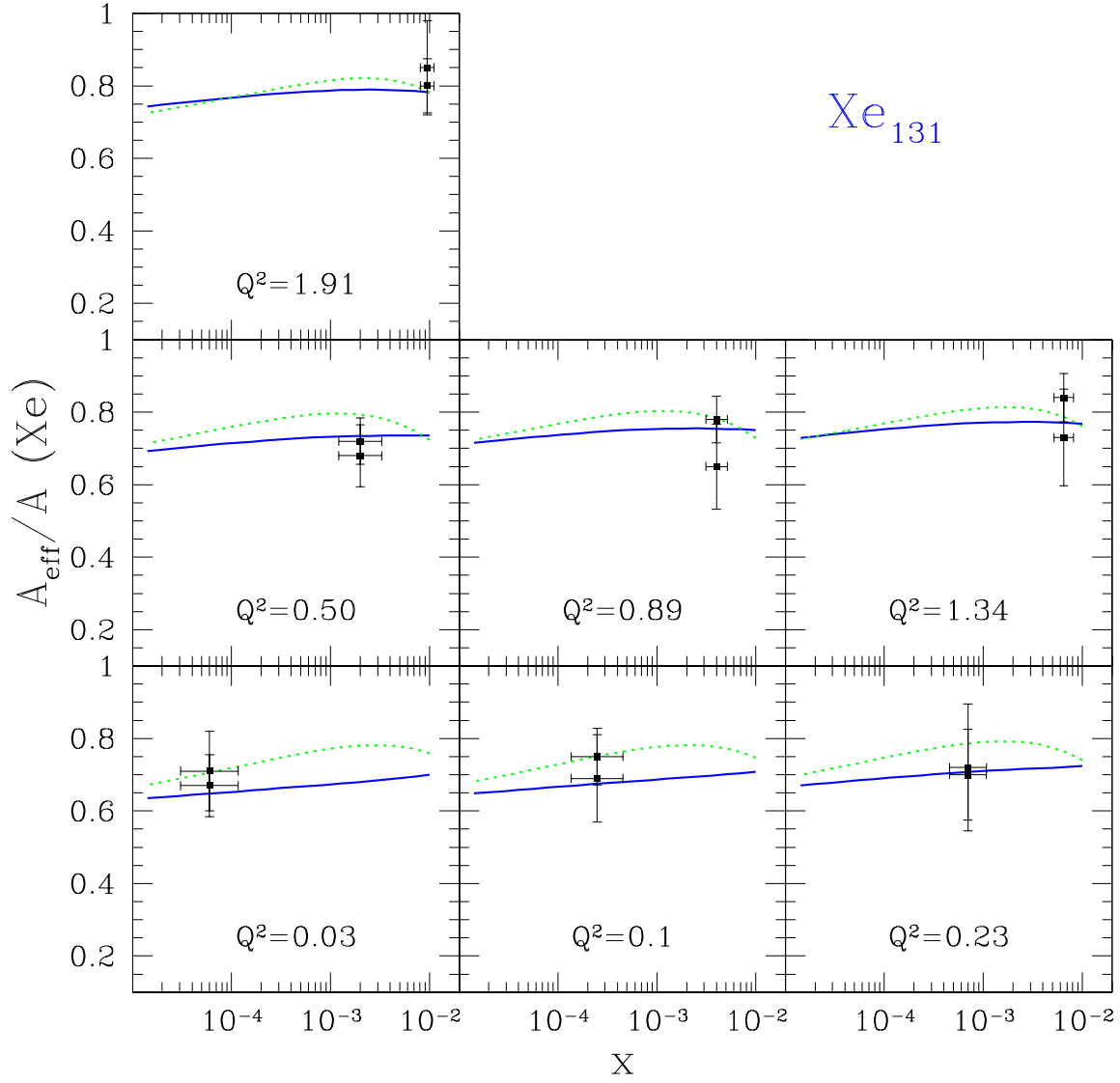


Figure 6:  $A_{\text{eff}}/A$  on a Xe target. Notation as in Fig. 5. Data from [26].

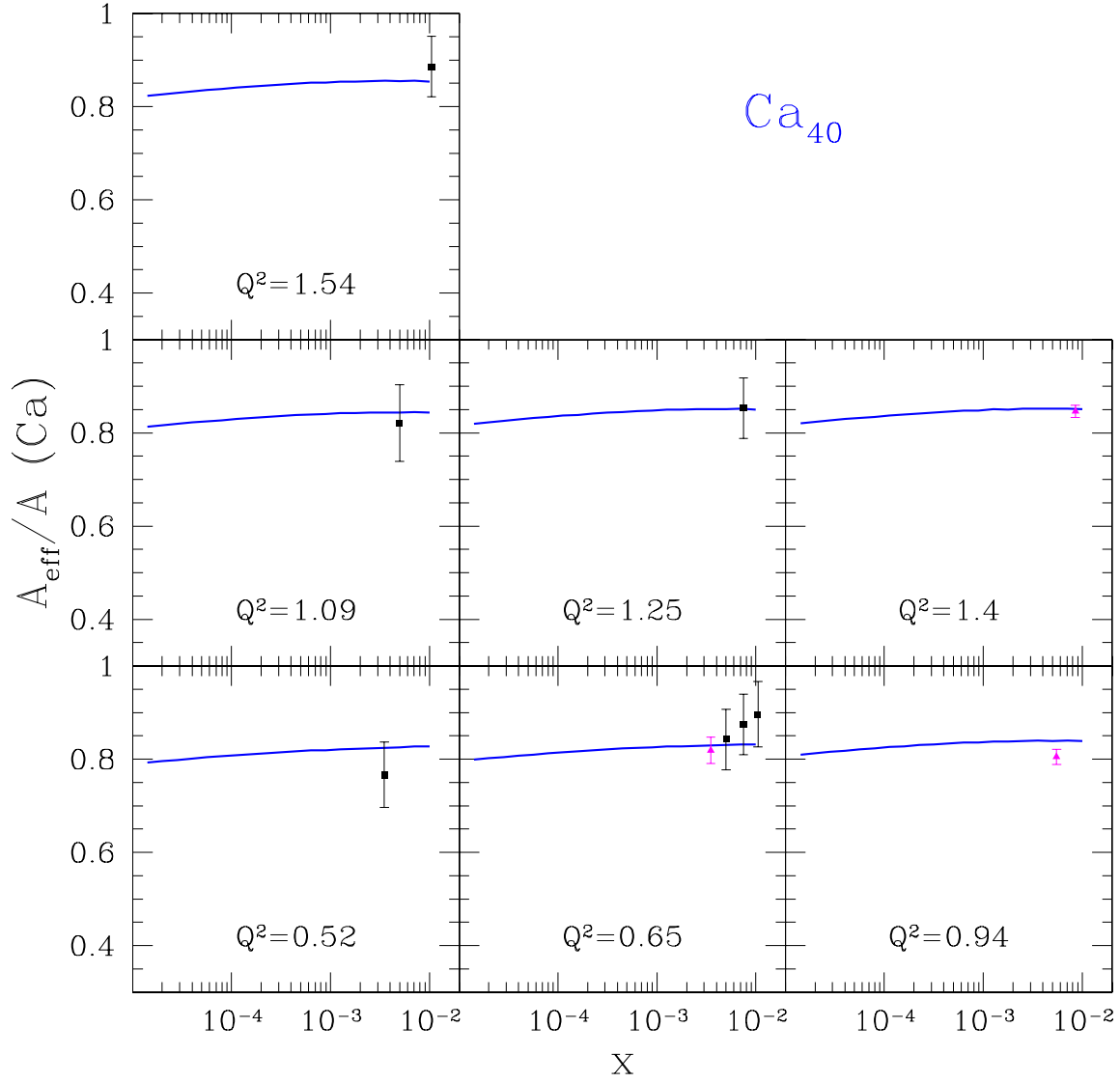


Figure 7:  $A_{\text{eff}}/A$  on a Ca target. Data from [27].

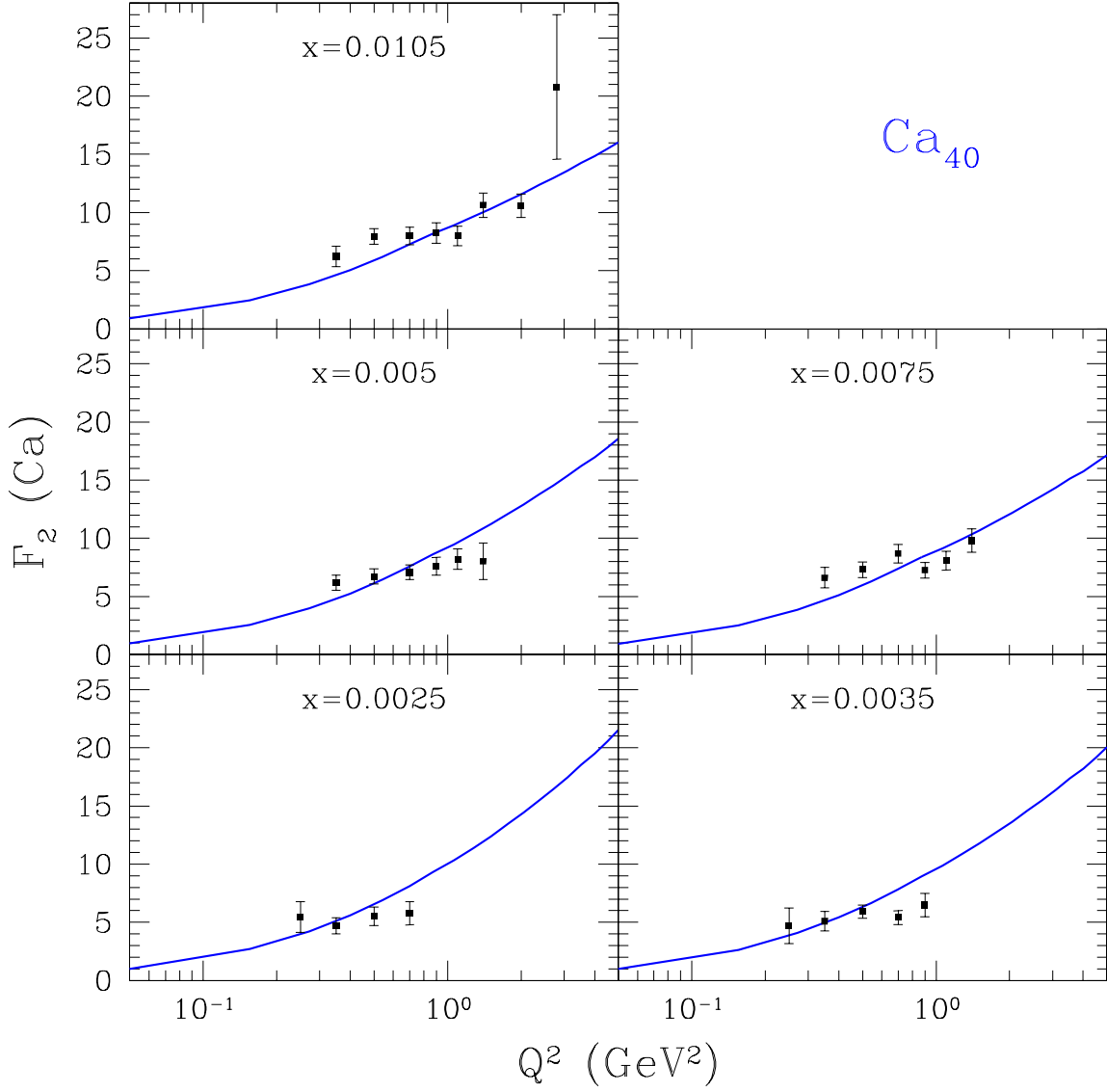


Figure 8:  $F_2$  on a Ca target. Data from [27].

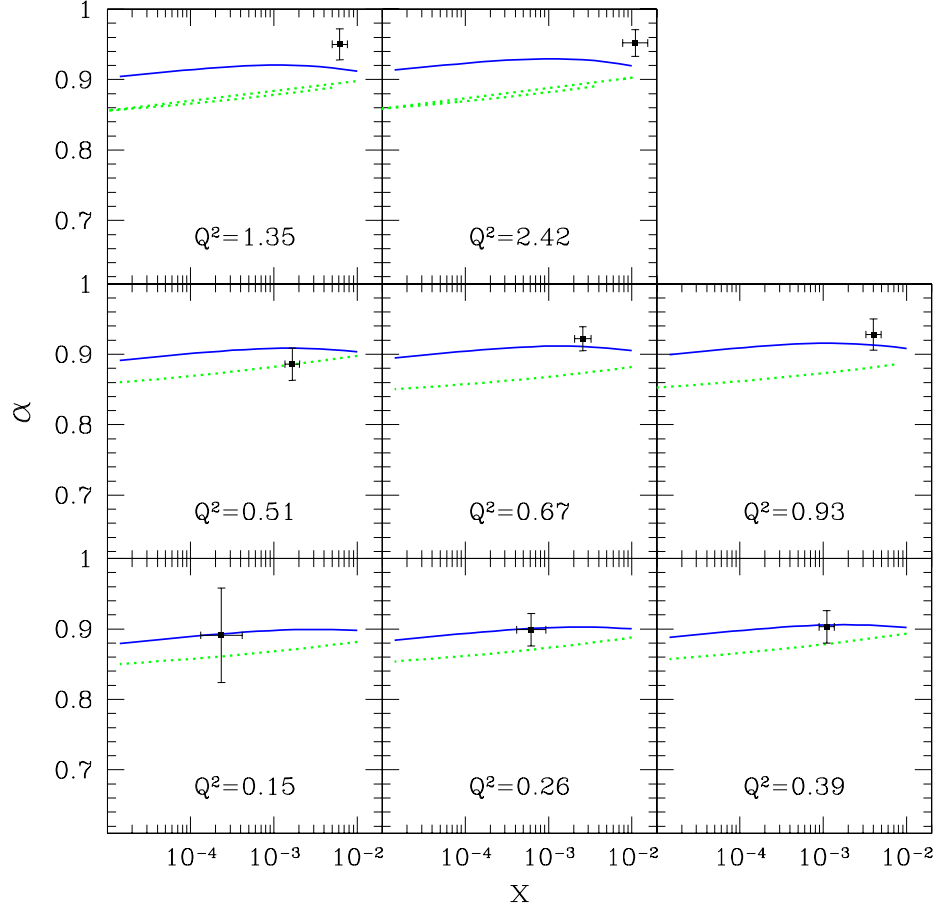


Figure 9:  $\alpha$  as a function of  $x$  for different values of  $Q^2$ . Notation as in Fig. 5. Data from [25].

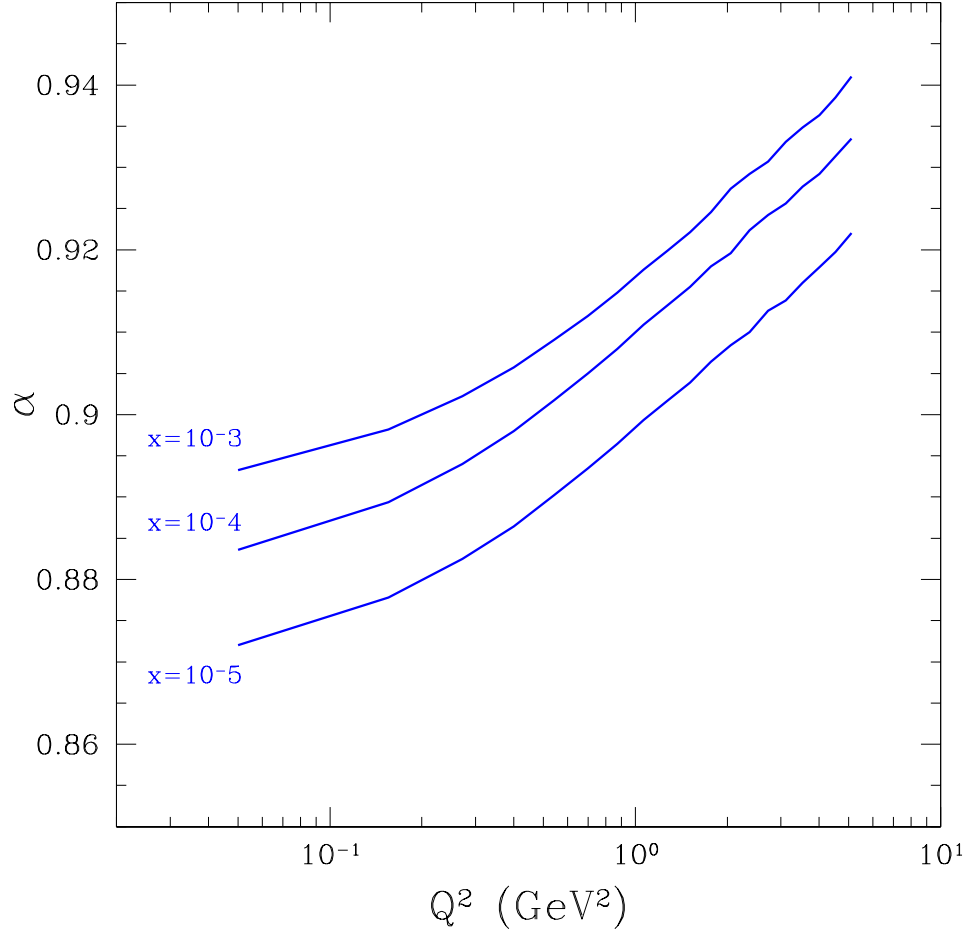


Figure 10:  $\alpha$  as a function of  $Q^2$  for fixed values of  $x$ . Prediction of our model including a secondary Regge contribution.



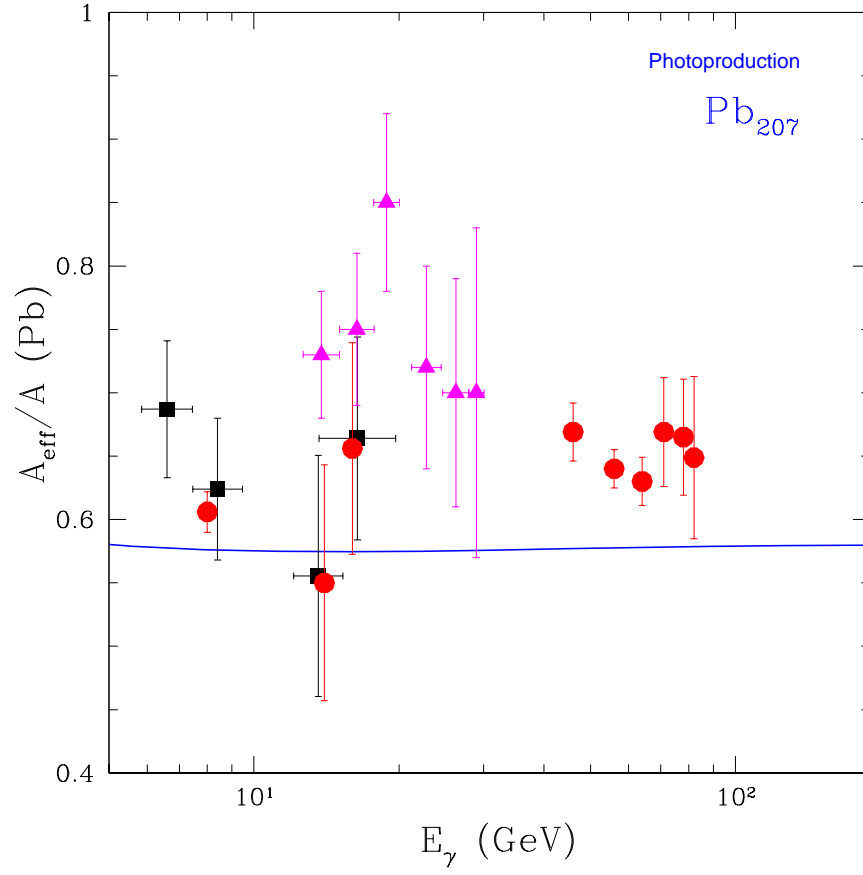


Figure 11: Photoproduction:  $A_{\text{eff}}/A$  as a function of  $\gamma$  energy for scattering on a Pb target. Data from [28].

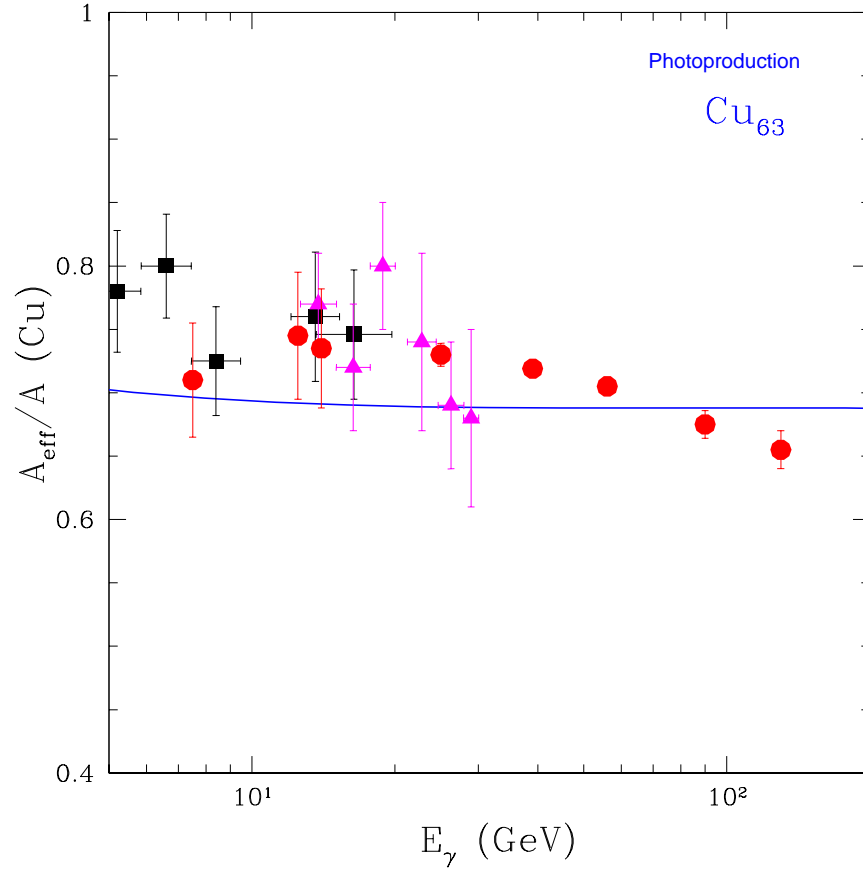


Figure 12: Photoproduction:  $A_{\text{eff}}/A$  as a function of  $\gamma$  energy scattering on Cu target. Data from [28].

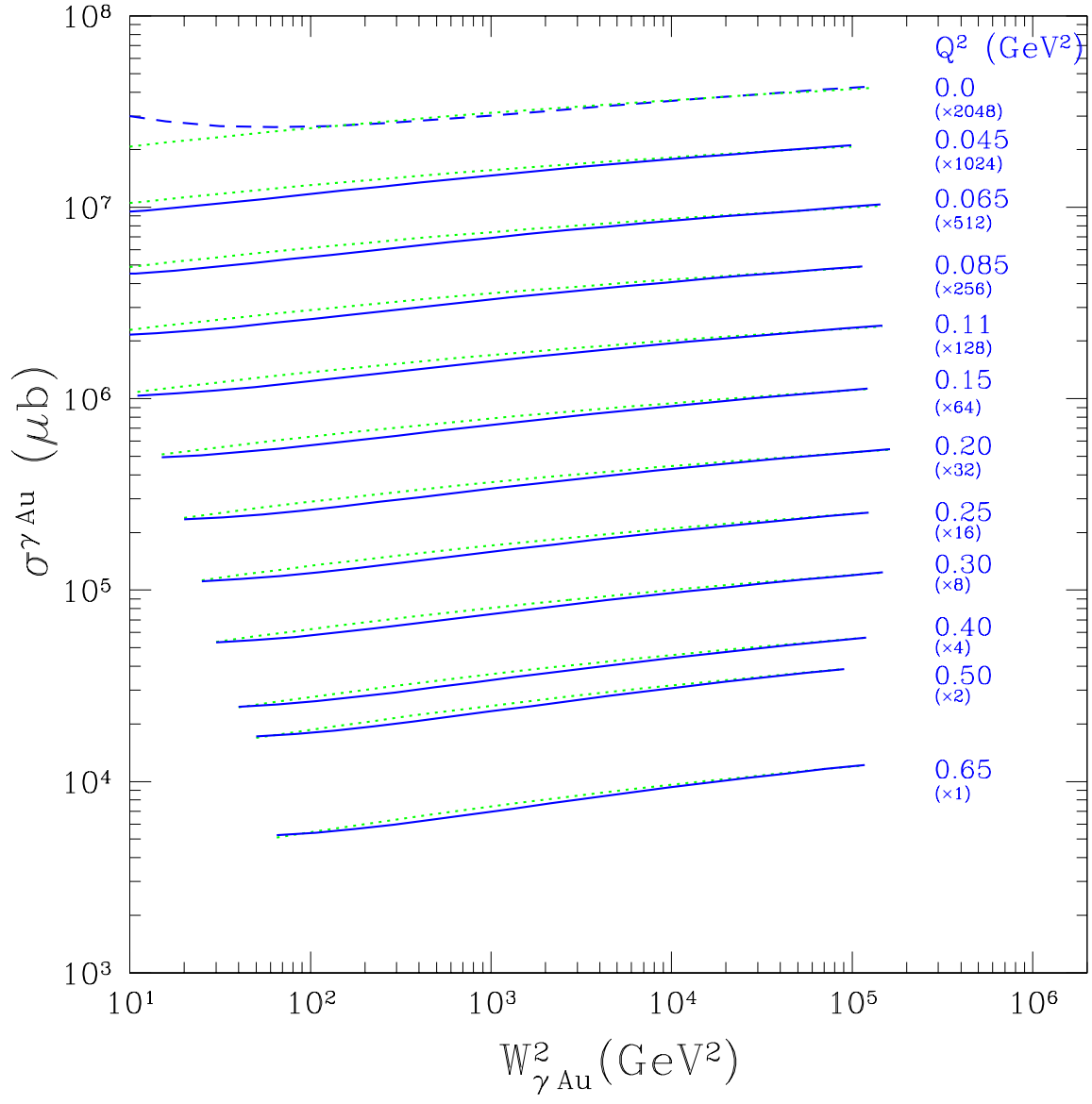


Figure 13: The predictions of our model for the DIS cross section on Au at very low  $Q^2$ . Notation as in Fig. 5.

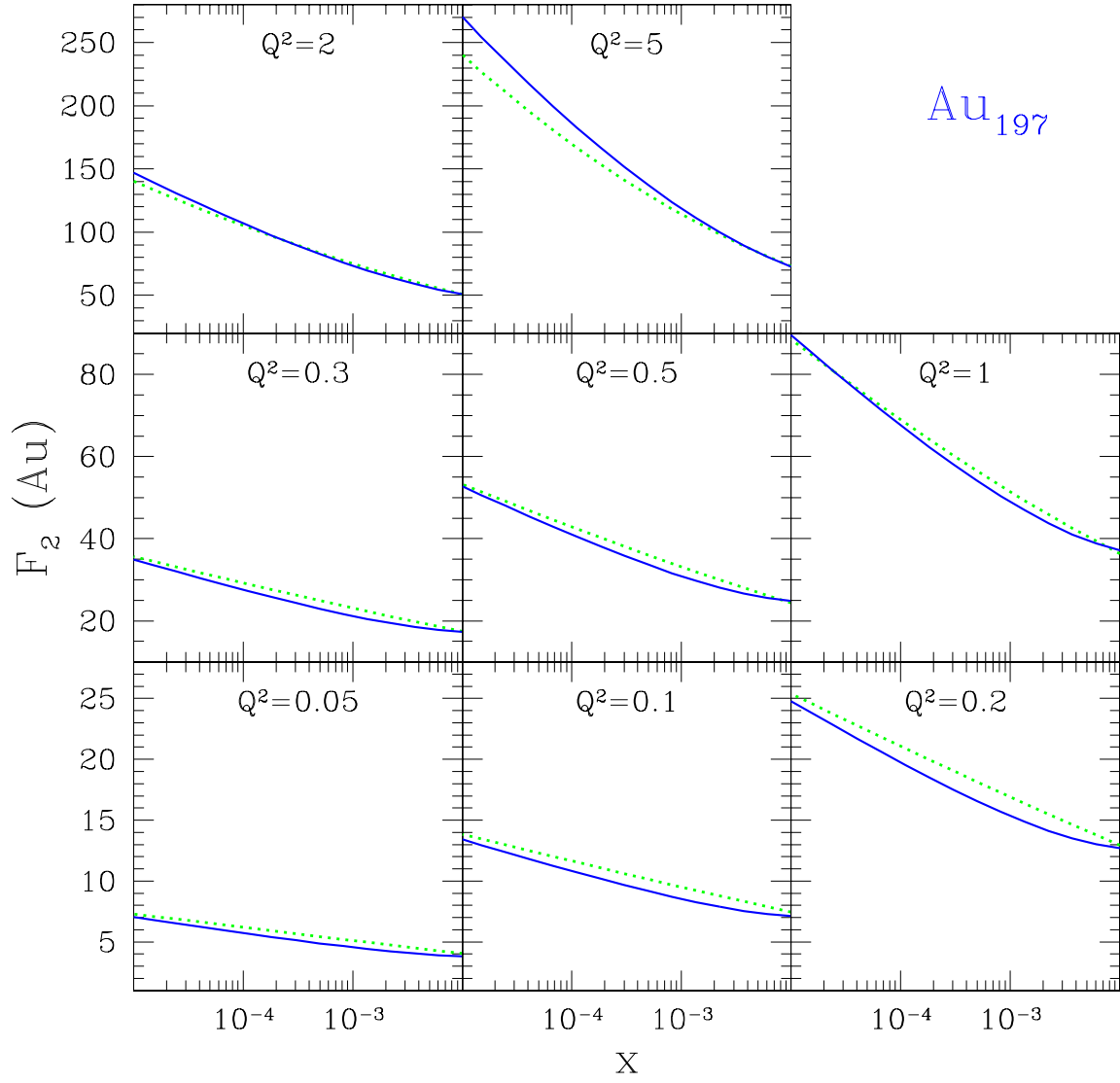


Figure 14:  $F_2$  for gold ( $A = 200$ ) as a function of  $x$  for fixed values of  $Q^2$ . Notation as in Fig. 5

Our main result, that we are successful in describing the photoproduction data for nuclear targets, is compelling and encourages us to suggest further measurements of photon - nuclei interactions. We stress that the Glauber approach for nuclear targets does not contain any additional assumptions, thus nuclear data can be used for clarifying the situation regarding our assumptions and fitting parameters.

This paper and our previous work [6], provide evidence that an approach based on the QCD dipole picture and on QCD saturation is successful in describing processes which traditionally have been associated with soft physics. They also reinforce the results obtained in Ref. [4] namely, that QCD saturation is a natural bridge between soft physics and conventional perturbative QCD.

## 7 Acknowledgments

We thank Nestor Armesto, Eran Naftali, and Anna Stasto for useful discussions. E.L. is indebted to the DESY Theory Division for their hospitality, while E.G. is grateful to the Department of Physics and Astronomy at UCI for their cordial support. M.L. thanks the Institute for Nuclear Theory at the University of Washington for its hospitality and the Department of Energy for partial support during the completion of this work. This research was supported in part by the GIF grant # I-620-22.14/1999, and by the Israel Science Foundation, founded by the Israeli Academy of Science and Humanities.

## References

- [1] ZEUS Collab., *Eur. Phys. J. C* **7**, (1999) 609; *Phys. Lett.* **B487** (2000) 53.
- [2] K. Golec-Biernat and M. Wüsthoff, *Phys. Rev.* **D59** (1999) 014017.
- [3] J. Bartels, K. Golec-Biernat and H. Kowalski, *Phys. Rev.* **D 66** (2002) 014001.
- [4] E. Gotsman, E. Levin, M. Lublinsky and U. Maor, *Eur. Phys. J. C* **27** (2003) 411.
- [5] J. Kwiecinski and L. Motyka, *Phys. Lett.* **B 462** (1999) 203; N. Timneanu, J. Kwiecinski and L. Motyka, hep-ph/0206130; *Eur. Phys. J.* **23** (2002) 513, hep-ph/0110409 ; M. Kozlov and E. Levin hep-ph/0211398 ; S. Bondarenko, M. Kozlov and E. Levin, hep-ph/0303118.
- [6] J. Bartels, E. Gotsman, E. Levin, M. Lublinsky and U. Maor, *Phys. Lett.* **B 556** (2003) 114.
- [7] Ia. Balitsky, *Nucl. Phys.* **B 463** (1996) 99; Yu. Kovchegov, *Phys. Rev.* **D60** (2000) 034008.
- [8] L. V. Gribov, E. M. Levin, and M. G. Ryskin, *Nucl. Phys.* **B 188** (1981) 555; *Phys. Rep.* **100** (1983) 1.
- [9] A.H. Mueller and J. Qiu, *Nucl. Phys.* **B 268** (1986) 427; J.-P. Blaizot and A.H. Mueller, *Nucl. Phys.* **B 289** (1987) 847.
- [10] L. McLerran and R. Venugopalan, *Phys. Rev.* **D 49** (1994) 2233; 3352; **D 50** (1994) 2225.
- [11] A. Donnachie and P. V. Landshoff, *Nucl. Phys.* **B 244** (84) 322, **B 267** (1986) 690; *Phys. Lett.* **B 296** (92) 227; *Z. Phys.* **C 61** (1994) 139; *Phys. Lett.* **B 437**, (1998) 408.
- [12] N. Armesto, *Eur. Phys. J. C* **26** (2002) 35.

- [13] E. Gotsman, E.M. Levin, M. Lublinsky, U. Maor and E. Naftali, [hep-ph/030210](#).
- [14] V. N. Gribov, *Sov. Phys. JETP* **30** (1970) 709.
- [15] A. H. Mueller, *Nucl. Phys.* **B 415** (1994) 373.
- [16] A. H. Mueller, *Nucl. Phys.* **B 335** (1990) 115.
- [17] N. N. Nikolaev and B. G. Zakharov, *Z. Phys.* **C 49** (1991) 607; E. M. Levin, A. D. Martin, M. G. Ryskin, and T. Teubner, *Z. Phys.* **C 74** (1997) 671.
- [18] J. Pumplin, D. R. Stump, J. Huston, H. L. Lai, P. Nadolsky, W. K. Tung, *JHEP* 0207 (2002) 012.
- [19] E. Gotsman, E. Levin, U. Maor, and E. Naftali, *Eur. Phys. J.* **C 10** (1999) 689; E. Gotsman, E. Levin and U. Maor, *Eur. Phys. J.* **C 5** (1998) 303; B. Badelek and J. Kwiecinski, *Z. Phys.* **C 43** (1989) 251; *Phys. Lett.* **B 295** (92) 263; *Phys. Rev.* **D 50** (1994) R4. 094011.
- [20] ZEUS Collab., DIS2000, preliminary.
- [21] ZEUS Collab, J. Breitweg et al., *Phys. Lett.* **B 487** (2000) 53.
- [22] H. G. Dosch, E. Ferreira and A. Krämer, *Phys. Rev.* **D5** (1994) 1992.
- [23] E. Gotsman, E. M. Levin and U. Maor, *Phys. Lett.* **B 309** (1993) 199.
- [24] N. Armesto, A. Capella, A. B. Kaidalov, J. Lopez-Albacete, C. A. Salgado, [hep-ph/0304119](#).
- [25] E665 Collaboration, M. R. Adams *et al.* *Z. Phys.* **C 67**, (1995) 403.
- [26] E665 Collaboration, M. .R. Adams *et al.* *Phys. Rev. Lett.* **68** (1992) 3266. *Z. Phys.* **C 67**, (1995) 403.
- [27] EMC Collaboration, P. Amaudruz et al., *Nucl. Phys.* **B 441** (1995) 3; M. Arneodo et al, *Phys. Lett.* **B 211** (1988) 493; *Nucl. Phys.* **B 333** (1990) 1.
- [28] D.O. Caldwell et al. *Phys. Rev. Letts.* **42** (1979) 553; E.A. Arakelian et al, *Phys. Letts.* **B 79** (1978) 143; D.O. Caldwell et al. *Phys. Rev.* **D 7**(1973) 1362.